

Optimization of Çayeli(Çbi) Grinding Circuit By Modelling And Simulation

L. Ergün, Ö. Gülsoy, M. Can & H. Benzer

Department of Mining Engineering, Hacettepe University, Ankara, Turkey

ABSTRACT: In this study, optimization of the ÇBİ grinding circuit after installation of tertiary crusher was carried out using modelling and simulation techniques. A detailed sampling survey was performed and size distributions of the samples were determined by the combination of wet sieving and cyclosizing down to 8.8/tm. Bond Work Index and breakage characteristics of the feed sample were determined by standard Bond test and drop weight test, respectively. After mass balancing studies, using the mass balanced data, the models for both ball mills and hydrocyclones were developed. The existing performance was predicted using only measured size distribution and tonnage of the fresh feed. The predicted size distributions, tonnages and cyclone parameters were in very good agreement with the measured data. The fineness and solids content of the flotation feed was %72.4 -36µm and 42.6% solids by weight respectively obtained during the survey were taken as target values in the simulation studies. The effects of feed rate and size distribution, solids content of cyclone feed, grindability of the ore, ball size, apex and vortex finder diameter were investigated by computer simulations. The results showed that performance of the existing circuit could be improved. Optimum apex and vortex finder diameters were found to be 75 mm and 125 mm, respectively. The fineness of the flotation feed could be increased and circulating load could be further decreased by using 20 mm balls in the secondary mill.

1 INTRODUCTION

Simulation of the grinding circuits using mathematical models of the mills and classifiers is a technique which is being used increasingly in comminution because of its low cost and its ability to consider many variables simultaneously. Its value depends on the accuracy of the models. The problems with these which encountered for several years are diminishing as experience with simulation is being gained in the design and optimisation of grinding circuits and models are being refined.

Simulation would provide the quantified information about the effects of the proposed changes on the circuit performance in terms of size distribution, solid and water flowrates etc. Such information could then be used to check the suitability of the existing equipment to the modified conditions, and for equipment selection. It could also be used to estimate the improvement expected in the downstream flotation circuit performance.

ÇBİ grinding circuit has been modified during the years to improve the performance. After installation

of single stage classification instead of double stage the annual capacity has increased to 1,000,000 tons. This has also improved control over classification and simplified the operation (Aksam and Mian, 2003). Then, to further improve the capacity and performance, a tertiary crusher has installed in the crushing circuit.

The aim of the study is to investigate optimum operating variables in ÇBİ grinding circuit using modelling and simulation techniques, after installation of tertiary crusher.

For this purpose sampling survey was carried around the circuit. After mass balancing, using the size distributions and tonnages, models for ball mills and hydrocyclones were developed. Finally, the effects of operating parameters on the circuit performance were investigated by computer simulations.

2. MODELS USED

For the ball mills and hydrocyclones, the models developed in Julius Kruttschnitt Mineral Research Center were used (Napier-Munn, et al, 1996)

Ball MM Model

Perfect mixing modelling approach is used for ball mill modelling (Lynch, 1977). The model considers a ball mill or a section of it as a perfectly stirred tank. Then, the process can be described in terms of transport through the mill and breakage within the mill.

Because the mill is perfectly mixed, a discharge rate, d_i , for each size fraction is an important variable in defining the product

$$p_i = d_i s_i$$

The equations for steady state operations are,

$$f_i - r_i s_i + \sum_{j=1}^i a_{ij} r_j s_j - d_i s_i = 0 \quad (1)$$

or, by substituting s_i with $\frac{p_i}{d_i}$,

$$f_i - r_i \frac{p_i}{d_i} + \sum_{j=1}^i a_{ij} r_j \frac{p_j}{d_j} - p_i = 0 \quad (2)$$

where,

- f_i Feed rate of size fraction i (M/h)
- p_i Product rate of size fraction i (t/h)
- a_{ij} The mass fraction of particle of size that appear at size i after breakage
- r_i Breakage rate of particle size i (h⁻¹)
- s_i Amount of size i particles inside the mill (t)
- d_i The discharge rate of particle size (h⁻¹)

If the breakage distribution function is known, calibrating the model to a ball mill involves the calculation of r_i / d_i values using the feed and product size distributions obtained under particular operating conditions. Where the size distribution of the mill content is available, breakage rates and discharge rates can be calculated separately.

Hydrocyclone Model

Hydrocyclone classifiers are modelled using the model developed by Nageswararao (Napier-Munn, et al, 1996). The model is based on efficiency curves for classifiers. The general form of the equation is presented below. This equation is capable of defining fish hook type efficiency curves.

$$E_{oa} = C \left[\frac{(1 + \beta \beta^* X)(\exp(\alpha) - 1)}{\exp(\alpha \beta^* X) + \exp(\alpha) - 2} \right] \quad (3)$$

where

- E_{oa} The actual efficiency expressed as the particles reporting to overflow
- C The proportion of feed particles which are subjected to the classifying action within a classifier ($= 1$ bypass)
- a A model parameter defining the sharpness of classification
- β A model parameter defining the fish hook
- β^* A dummy parameter introduced to the model to preserve the definition of d_{50c} (i.e. $d = d_{50c}$ when $E = (1/2)C$)
- X $\frac{d_i}{d_{50c}}$
- d_i Particle size
- d_{50c} The corrected cut size which is defined as the size which divides equally between underflow and overflow due to classification only

Nageswararao developed a number of empirical equations defining the relationship between operating and geometrical variables of hydrocyclones, and model parameters including d_{50c} and water recovery (Napier-Munn, et al, 1996). There are also four calibration constants in the equations which are used to define material characteristics. The model could be used to predict cyclone inlet pressure and roping conditions when operating variables are changed. The calibration of hydrocyclone model involves the calculation of the best fit values a , β , d_{50c} and C to the plant data. The calibration constants defining the dependence of d_{50c} capacity, water recovery and volumetric recovery on operating geometrical variables are also determined. If fish hook behaviour does not exist, then β is taken as equal to one.

When a cyclone model is calibrated, material characteristics in relation to its behaviour in classifying circuit is determined. The parameters fitted to the experimental data are material specific. After the calibration, the effects of all operating and geometrical variables on the separator performance could be investigated by simulation (Napier-Munn, et al, 1996).

2. SAMPLING SURVEY AND DATA ANALYSIS

A detailed sampling survey was performed at 132 dmtp/h (dry metric ton per hour). Samples were taken from each stream in the circuit and solids content of all samples were determined. The simplified flowsheet with the marked sampling points on it are given in Figure 1 and the geometrical parameters of

the equipments and the measured data are presented in Table 1.

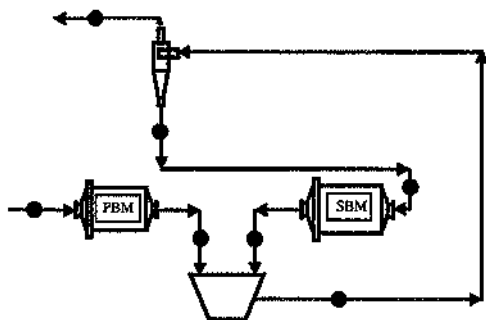


Figure 1. Simplified flowsheet of ÇBI grinding circuit and sampling points.

Table 1. Main operating and design conditions for the sampling survey

	Primary Ball Mill	Se-on-dary Ball Mill
Mill Outer Diameter (mm)	3200	4400
Mill Length (mm)	4300	7200
Liner Thickness (mm)	100	50
Mill Speed	17.4	15.4
Critical Speed (Cs)	24.7	20.55
% Cs	70.5	74.9
Ball Size(mm)	100	40
Power (kW)	560	2160
Hydrocyclone		
Diameter (mm)	371.2	
Inlet Diameter (mm)	152	
VF diameter (mm)	130	
VF length (mm)	276	
Apex diameter (mm)	70	
Cylinder length (mm)	360	
Cone angle (°)	10	

Feed Tonnage (wet)	135.66-136
PBM (kW)	511.57-512
SBM (kW)	1958.14-1958
Cyclone Pressure (bar)	0.85
Cyclone Feed Density (t/m ³)	1.85
Cyclone Feed % Solids	61.74-61.7
Flotation Feed % Solids	41.47
PBM Water Addition (m ³ /h)	28.95-29.0

Sump Water Addition
(m³/h)

132.08-132.0

Size distributions of the samples were determined by the combination of wet sieving and cyclizing down to 8.8µm. Bond grindability and work index of the plant feed were determined using standard Bond test for 74 micron test sieve. Bond index of the feed sample was measured as 9.70 kWh/t. Breakage distribution of the material was determined using drop weight test apparatus built at Hacettepe University Laboratories. The breakage function of the mill feed is given in Figure 2.

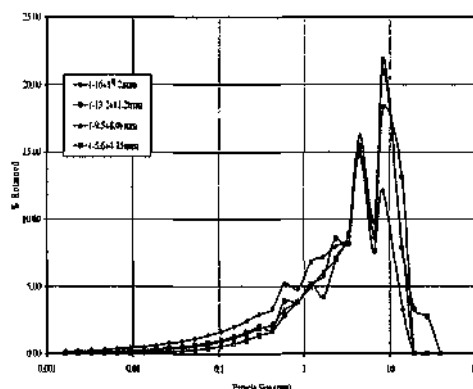


Figure 2. Breakage Functions of different size fractions of the mill feed

The size distribution and breakage data were used for the mass balancing studies.

3. MASS BALANCING STUDIES

In any sampling operation, the occurrence of some errors are inevitable. These errors result from dynamic nature of the system, physical conditions at particular point, random errors, measurement errors and human errors. Mass balancing is the key to eliminate these errors statistically. Mass balancing of the raw data was accomplished by using JKSimMet software.

During the mass balancing studies, all the flow rates and the percent solids around the circuit were calculated as given in Figure 3. The results of the size distributions of raw and adjusted data of the streams around the circuit are given in Figure 4.

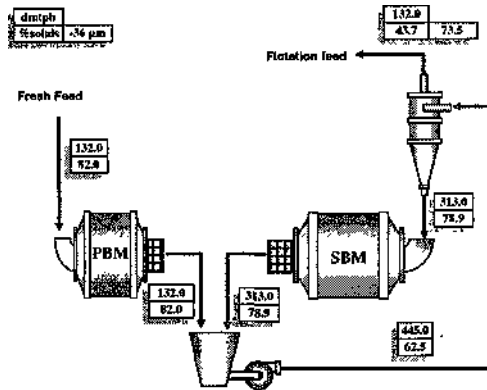


Figure 3. The simplified flowsheet after mass balancing

The actual and corrected performance curves of the hydrocyclone are given in Figure 5. The hydrocyclone was operating with 30 % water recovery to underflow and the actual cut size was about 40 *µm*.

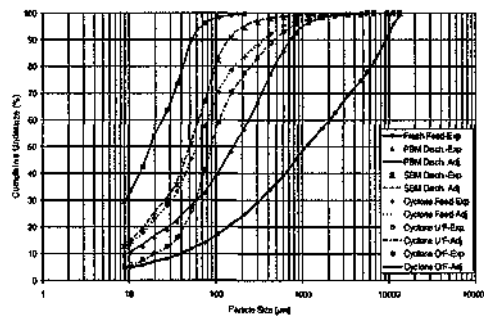


Figure 4. The measured and calculated size distributions

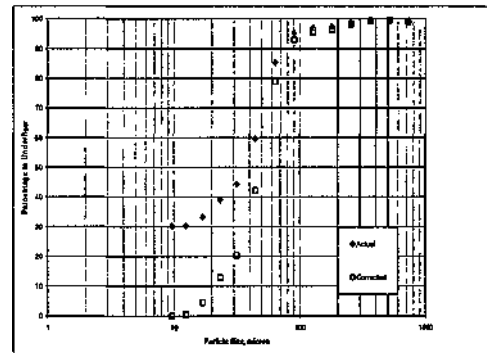


Figure 5. The actual and corrected performance curves of the hydrocyclone

4. MODELLING AND SIMULATION

For the calculation of model parameters, the mass balanced data obtained from the survey were used. For the ball mills, using drop weight breakage function, r/d knots were calculated for the existing operating conditions. For the hydrocyclones, the model parameters in Nageswararo model were calculated. Average of the individual apex diameters of the cyclones were used. JKSimMet software were used for the calculation of model parameters.

Model parameters for ball mills and hydrocyclones are given at Table 2 and 3, respectively.

Table 2. r/d knots for the ball mills

primary ball mill		secondary ball mill	
size(mm)	$\ln(r/d)$	size(mm)	$\ln(r/d)$
0.03	-1.38	0.03	-1.91
0.2	-0.01638	0.08	0.5595
1.5	3.99	0.2	2.3
15	12.03	1	4.2

Table 3. Model parameters for the hydrocyclone.

KD0 (d50)	6.45E-05
KQ0 (Capacity)	353.19
KV1 (Volume split)	8.99
KW1 (Water split)	6.34
a	1.59
3	0.7796

The models fitted very good to the data and were found to be convenient for simulation studies. Then, using these models and by entering only tonnage and

size distribution of the fresh feed, the size distributions and mass flow rates were calculated.

In Figure 6, simulated and mass balanced size distributions are presented. As can be seen from the figures, the simulated size distributions were in a very good agreement with the mass balanced data. The cyclone operating pressure and tonnages of the streams were also very well predicted. The detailed results for the simulation of existing condition are given in Table 4.

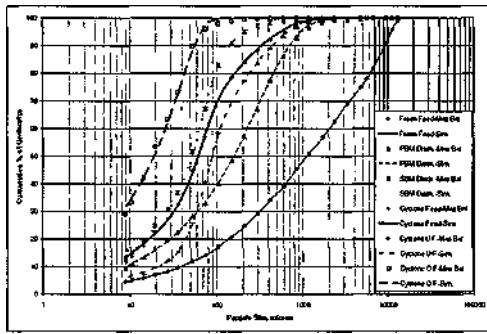


Figure 6. The simulated and mass balanced size distributions around the circuit

Table 4. The detailed results for the simulation of existing condition.

	PBM FEED		PBM DISCHARGE	
	Mass Bal	Sim	Mass Bal	Sim
Solids [tph]	132	132	132	132
Solids [%]	80	80	80	80
% Passing 36µm	9.57	9.57	22.56	22.38
80.0% Pas. (f/ft)	6130	6130	469	455
SBM DISCHARGE		CYCLONE FEED		
	Mass Bal	Sim	Mass Bal	Sim
Solids [tph]	313.01	313.09	445	445.07
Solids [%]	78.9	77.9	62.2	62.5
% Passing 36µm	36.84	36.53	32.59	32.33
80% Pas. (am)	99	98	165	163

	CYCLONE O/F		CYCLONE U/F	
	Mass Bal	Sim	Mass Bal	Sim
Solids [tph]	132	132	313.01	313.09
Solids [%]	43.7	42.6	78.9	77.9
% Passing 36µm	73.24	72.44	15.43	15.42
80 % Pas (fim)	41	43	249	240

	Meas	Sim
Corrected dsn (mm)	0.04934	0.05000
Cyclone pressure (bar)	0.85	0.84
Water split to O/F ($^{\circ}$)	65.99	66.7

As the simulation of existing condition was found to be successful, then various alternatives for the grinding circuit were evaluated.

4.1. Effect of feed rate

The effect of feed rate was investigated in the range of 132-160 dmtph.

The effect of feed rate on circulating load tonnage and primary ball mill discharge fineness are shown in Figure 7.

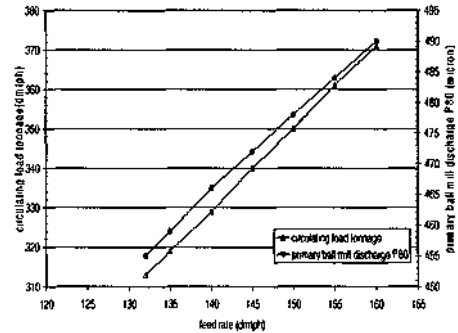


Figure 7. The effect of feed rate on circulating load tonnage and primary ball mill discharge fineness

The results showed that circulating load tonnage increases with increasing feed rate. The circulating load ratio decreases from 237% for 132 dmtph feed rate to 231% for 160 dmtph.

Primary ball mill discharge became coarser with the increase in feed rate. P80 sizes for the 132 dmtph feed and 150 dmtph are 455/µm and 478/µm, respectively.

The effect of feed rate on cyclone operating pressure and secondary ball mill discharge fineness are shown in Figure 8.

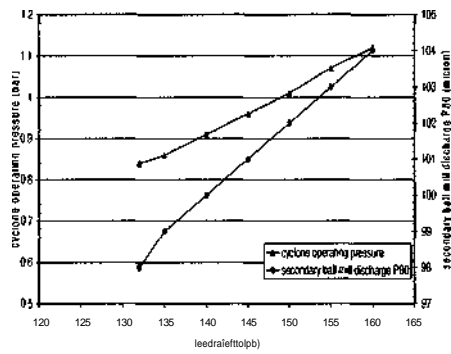


Figure 8. The effect of feed rate on cyclone operating pressure and secondary ball mill discharge fineness

As expected, an increase in feed rate causes an increase in cyclone operating pressure. P80 of secondary ball mill discharge slightly increased from 98/ μ m to 104/ μ m with the increase of feed rate from 132 dmtph to 160 dmtph.

The effect of feed rate on cyclone feed P80 and % solids are shown in Figure 9. As can be seen from the figure, both values increased with increasing feed rate. For the feed rates above 150 dmtph, cyclone feed % solids should increase to over 63.5% by weight (28.3% solids by volume) to obtain a flotation feed having 42.6% solids by weight. This can be considered as a limit for a reliable cyclone operation.

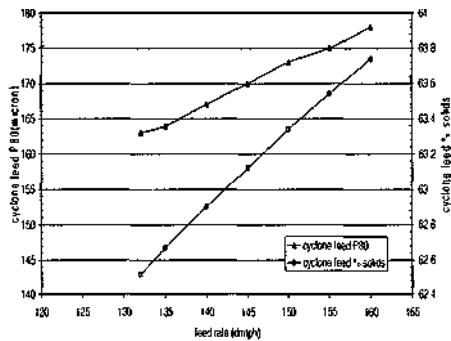


Figure 9. The effect of feed rate on cyclone feed P80 and % solids

The effect of feed rate on flotation feed P80 and % passing 36/ μ m are presented in Figure 10.

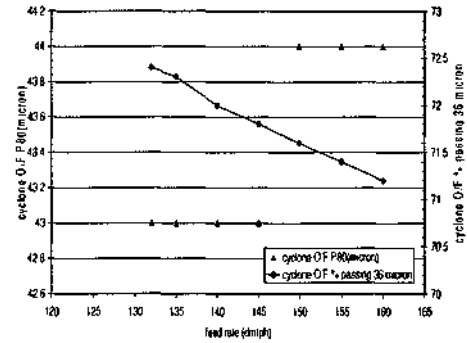


Figure 10. The effect of feed rate on flotation feed fineness

For the feed rate up to 145 dmtph P80 of the flotation feed was 43/ μ m, above this feed rate, P80 increased only 1 μ m. The amount of material passing 36/ μ m varies between 71 and 72.4%.

4.2. Effect of cyclone feed % solids

The effect of cyclone feed % solids was investigated in the range of 61-63.5%. The feed rate was kept constant at 132 dmtph.

The effect of cyclone feed % solids on circulating load tonnage and secondary ball mill discharge fineness are shown in Figure 11.

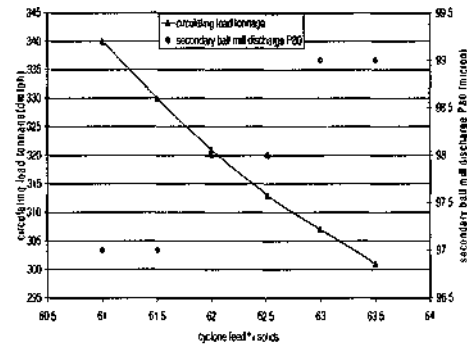


Figure 11. Effect of cyclone feed % solids on circulating load tonnage and secondary ball mill discharge fineness

As the cyclone feed % solids increases, circulating load decreases. Each 0.5% increase in cyclone feed % solids increased fineness of secondary ball mill discharge about 1 μ m. It can be concluded that secondary ball discharge did not significantly affected by cyclone feed density.

The effect of cyclone feed % solids on corrected d_{50} and operating pressure of the cyclone are given in Figure 12.

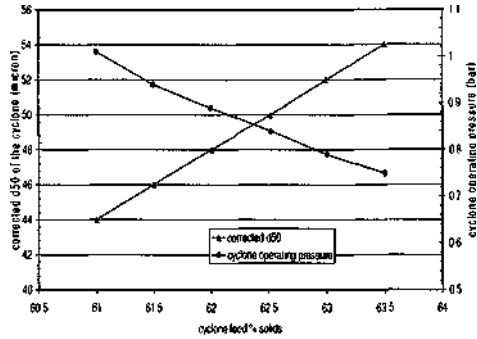


Figure 12. Effect of cyclone feed % solids on d_{50} and operating pressure of the cyclone

Increasing feed density increases cut size, while decreases pressure due to decrease in cyclone underflow tonnage. The change in the d_{50} is significant and it was 44 μm for 61% and increased 2 μm for each 0.5% increase in cyclone feed % solids. Both cyclone feed and underflow became coarser with the increase in cyclone feed % solids. This is illustrated in Figure 13.

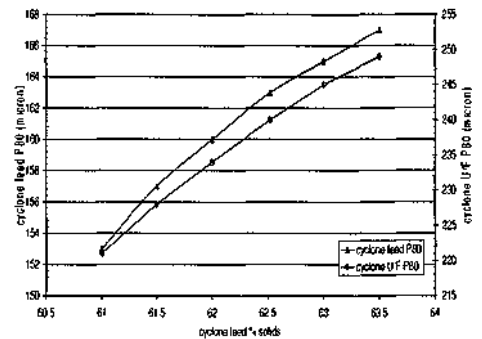


Figure 13. Effect of cyclone feed % solids on P80 of cyclone feed and underflow

The effect of cyclone feed % solids on flotation feed P80 and % passing 36 μm , and on flotation feed and cyclone underflow % solids are presented in Figure 14 and 15, respectively.

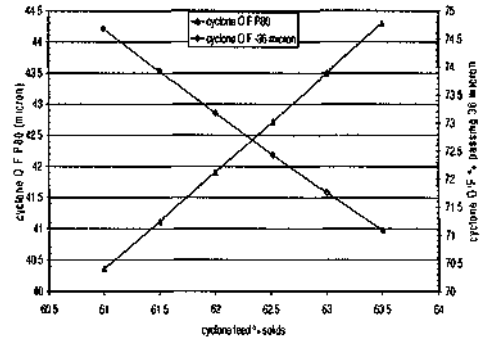


Figure 14. The effect of cyclone feed % solids on flotation feed fineness

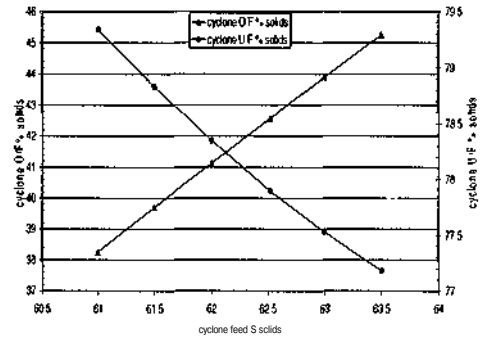


Figure 15. The effect of cyclone feed % solids on flotation feed and cyclone underflow % solids

The flotation feed became coarser as the cyclone feed density increased. Therefore, to keep flotation feed fineness constant, cyclone feed density should strictly be controlled. On the other hand, as it can be seen from Figure 15, there is a margin for decreasing cyclone feed density to reduce flotation feed density while keeping it in acceptable limits. In this case, it could be possible to increase the fineness of flotation feed when necessary.

4.3. Effect of size distribution of the fresh feed.

The effect of size distribution as investigated using the size distributions of samples taken during the sampling surveys and for the size distribution of fresh feed before installation of tertiary crusher.

The P80 sizes of the samples were between 5.68 mm and 7.20 mm during the surveys. Simulation studies showed that this variation did not effect the performance significantly. The only remarkable effect was on primary ball mill discharge and for the finest feed, P80 of which was 446 μm while for the coarsest it was 482 μm .

These size distributions are shown in Figure 16 and summarized in Table 5.

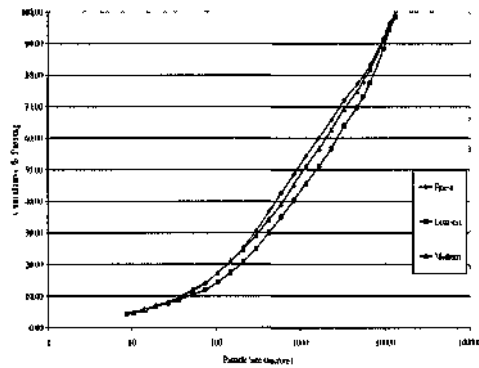


Figure 16. Fresh feed size distributions used in simulation studies

Table 5. Fresh feed size distributions used in simulation studies.

	finest	medium	coarsest
F90(mm)	9.18	10.53	13.20
F80 (mm)	6.13	7.00	8.15
F50 (mm)	1.11	1.31	1.58
F20(mm)	0.14	0.15	0.17

The effect of feed size distribution on circulating load and corrected d_{50} of the cyclone and primary and secondary ball mill discharge finenesses are shown in Figure 17 and 18, respectively. The effect of feed size distribution on cyclone pressure was very small therefore was not given in the figures.

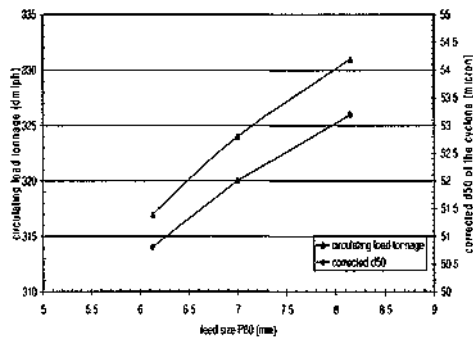


Figure 17. Effect of feed size distribution on circulating load and corrected d_{50}

Circulating load increased from 317 dmtp to 331 dmtp from the finest to coarsest feed and the corrected d_{50} increased from 51 / μ m to 53 / μ m.

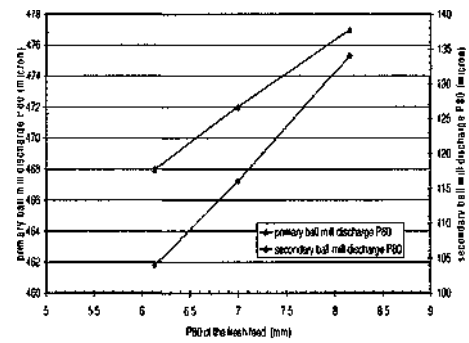


Figure 18. Effect of feed size distribution on primary and secondary ball mill discharge P80 sizes

The effect of feed size on P80 of the mill discharges was significant. Both mill discharges became coarser. The effect was more pronounced for secondary ball mill discharge.

Similar comments can be made for P80 of the cyclone feed and underflow which are shown in Figure 19.

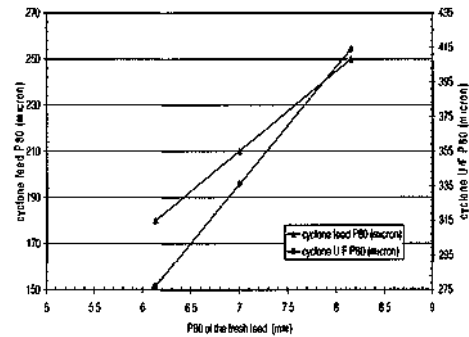


Figure 19. Effect of feed size distribution on cyclone feed and underflow P80 sizes

The effect of feed size distribution on cyclone feed and underflow % solids are shown in Figure 20. Both values increased about 1% within range studied.

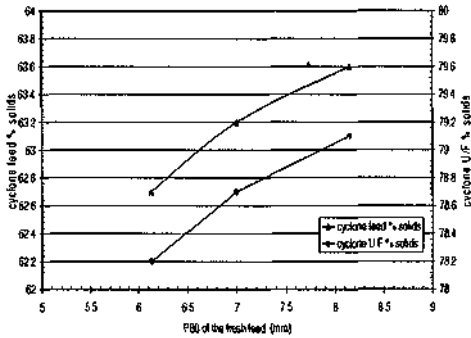


Figure 20. Effect of feed size distribution on cyclone feed and underflow % solids

The effect of feed size distribution on flotation feed P80 and % passing 36 μ m is exhibited in Figure 21.

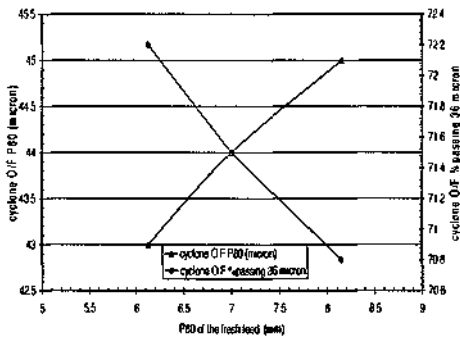


Figure 21. Effect of feed size distribution on flotation feed fineness.

As can be seen from Figure 21, flotation feed became coarser with coarser feed. However, the coarser size distributions tested can only be expected in any failure in tertiary crusher and serious blockage and material handling problems in the fine screening. Another simulation was run for the coarsest feed to increase the flotation feed fineness. In this case, cyclone feed density was decreased. The flotation feed % solids decreased to 41% solids by weight and hence % passing 36 μ m was increased to 71.7%.

4.4. Effect of grindability of the fresh feed

During surveys the Bond indices of the ore were found to be almost constant as 9.70 kWh/t and 9.55 kWh/t. In an earlier study, grindabilities of different ore types were also measured (Ergin et al., 2000). The highest Bond index was 10.46 kWh/t and the lowest was 8.68 kWh/t. Therefore, the effect of

grindability of the ore was investigated for these extremes and the grindability of this survey. Within the range studied, the effect of grindability was found to be minimum.

4.5. Effect of cyclone apex and vortex finder diameter

The effect of apex diameter on circulating load tonnage for different vortex finder diameters is shown in Figure 22.

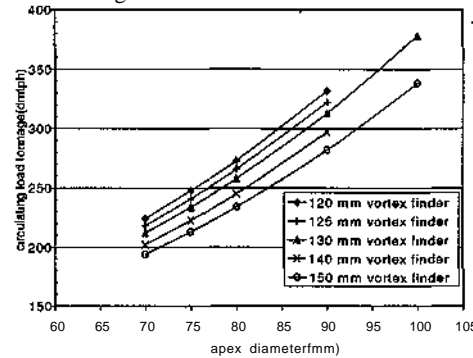


Figure 22. Effect of apex diameter on circulating load tonnage.

As can be seen from Figure 22, as apex diameter increases the circulating load increases for all vortex finders. The circulating load for the larger vortex finder diameters is less than smaller one. Since the effect of apex diameter is very pronounced, correct selection of it would be the key for successful operation.

The effect of apex diameter on secondary ball mill discharge fineness is shown in Figure 23.

P80 size of the secondary ball mill discharge increases as apex diameter increases. However, no discernible trend was observed for different vortex finder diameters.

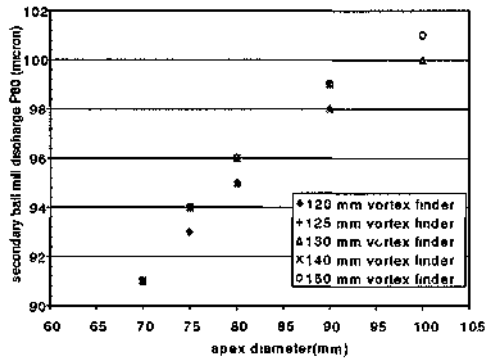


Figure 23. Effect of apex diameter on secondary ball mill discharge fineness.

The effect of apex diameter on cyclone feed fineness is given in Figure 24. As apex diameter increases, P80 of the cyclone feed decreases. For the same apex diameter, increasing vortex finder diameter gives a coarser cyclone feed.

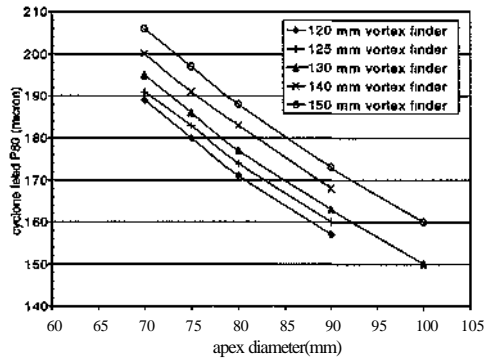


Figure 24. Effect of apex diameter on cyclone feed fineness.

The effect of apex diameter on cyclone feed solids is shown in Figure 25.

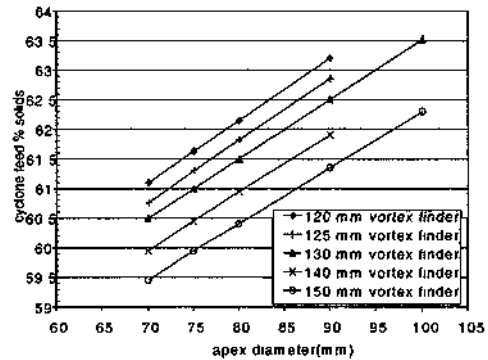


Figure 25. Effect of apex diameter on cyclone feed % solids

Cyclone feed % solids should be increased to obtain same flotation feed % solids for larger apices. For the same apex diameter, the difference between the largest and the smallest vortex finder is about 1.5% solids.

The effect of apex diameter on corrected d_{50} of the cyclone is shown in Figure 26.

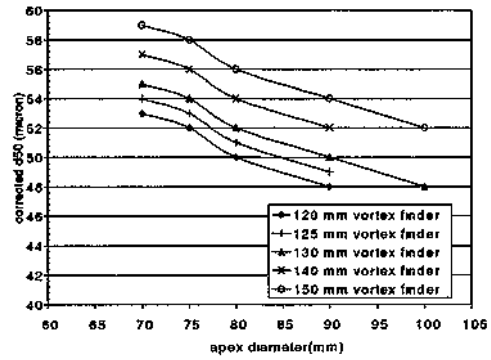


Figure 26. Effect of apex diameter on corrected d_{50}

As expected, an increase in apex diameter increases the corrected d_{50} value. Cyclone operating pressure increases with the increasing apex diameter (Figure 27).

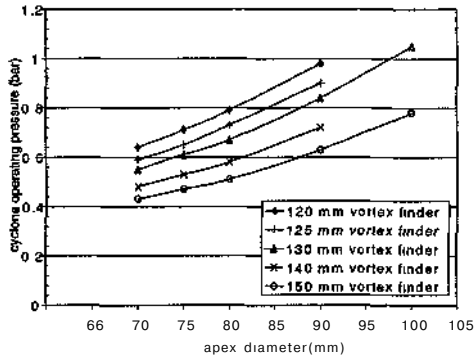


Figure 27. Effect of apex diameter on operating pressure of the cyclone

The effect of apex diameter on cyclone underflow fineness and % solids are shown in Figure 28 and 29, respectively.

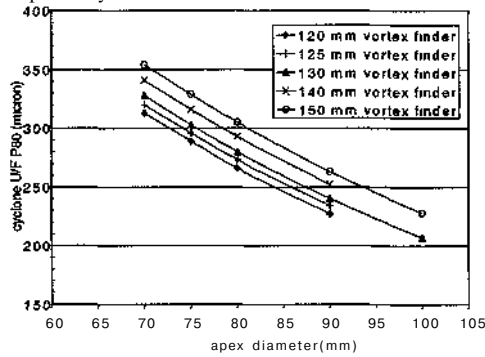


Figure 28. Effect of apex diameter on cyclone underflow fineness

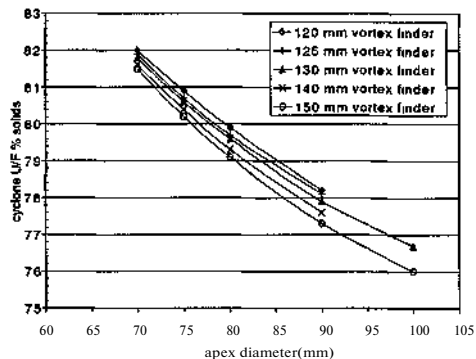


Figure 29. Effect of apex diameter on cyclone underflow % solids.

Cyclone underflow became finer with the increasing apexes due to increasing bypass to

underflow. For 70 mm and 90 mm apexes, the change in P80 values were in the order of 90 μ m. The cyclone underflow % solids sharply increases with the decreasing apex diameter. Although during simulations no roping was observed for the 70 mm apexes, cyclone underflow % solids were near to roping condition. It is evident that apex diameter smaller than 90 mm (base condition) would be useful.

The effect of apex diameter on flotation feed fineness is shown in Figure 30 and 31. From both figures, it can be seen that for the different apexes flotation feed fineness did not change significantly. For a given apex diameter as the vortex finder diameter increases, flotation feed becomes coarser.

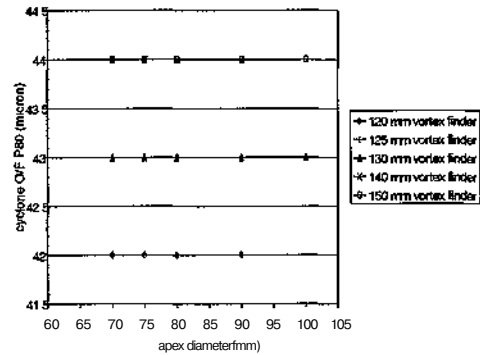


Figure 30. Effect of apex diameter on flotation feed P80

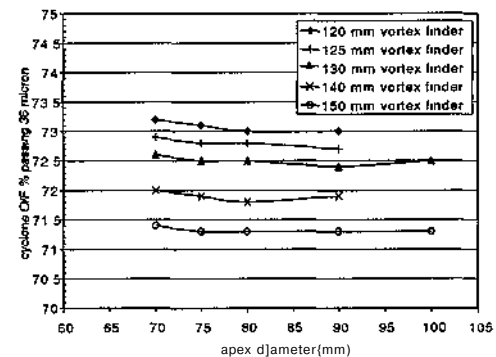


Figure 31. Effect of apex diameter on flotation feed % passing 36 /mi

4.6. Effect of ball load and ball size

The measured volumetric ball loads for primary and secondary ball mills during surveys were 43% and

35%, respectively. Ball load in the primary ball mill was not changed in simulations. According to power calculations volumetric ball load in the secondary ball mill could be increased to 42%. Therefore, simulations were run for 40% and 42% volumetric ball load. Increasing ball load would increase the flotation feed fineness marginally from 72.4% -36/µm to 73.1% and 73.2% for 40% and 42% load, respectively. But practically at the plant conditions it is not possible to load the mill up to these values.

Using Bond formula, the top size of the balls for primary ball mill and secondary ball mill were calculated as 65 mm and 15 mm, respectively. However, considering the coarsest feed to the primary ball mill which is given in Figure 32, it should be larger than 70 mm. Therefore, only the effect of 20 mm ball size in the secondary ball mill was investigated without changing the ball size in PBM. All the conditions were kept constant as in the sampling survey, except ball size.

The performance of the circuit is shown in Figure 32.

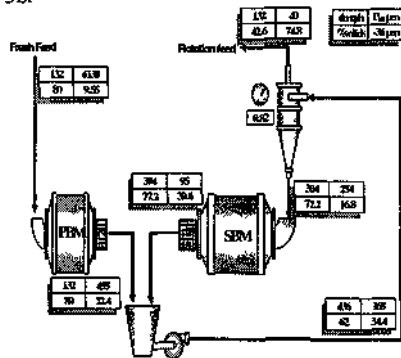


Figure 32. The performance of the circuit using 20 mm balls in secondary ball mill

The results showed that using 20 mm ball in the secondary ball mill would improve the performance of the circuit.

5. CONCLUSIONS

Modelling of ball mills and hydrocyclone were performed using the data collected from ÇBİ grinding circuit. The models predicted existing performance very well as given in Figure 4.

The results showed that performance of the existing circuit for 132 dmtph could be improved. Optimum apex and vortex finder diameters were found to be 75 mm and 125 mm, respectively. In this

case, circulating load ratio would be decreased from 2.4 to 1.8. It is suggested that both of them should be replaced after 10 mm wear. The fineness of the flotation feed could be increased and circulating load could be further decreased by using 70 mm balls in the primary ball mill and 20 mm balls in the secondary mill. In this case, fineness of flotation feed would be 75% -36/µm.

Acknowledgment

The authors would like to thank ÇBİ Management for the financial support and for the permission to publish this paper, and also to Mill Staff for their efforts during the studies at Çayeli.

REFERENCES

- Lynch, A.J. 1977. *Mineral crushing and grinding circuits: their simulation, optimisation, design and control*. Elsevier. 340pp.
- Napier-Munn, T.J., Morrell, S., Morrison, R.D. & Kojovic, T. 1996. *Mineral comminution circuits: their operation and optimisation*. JK/MRC. 413pp.
- Ergün, Ş.L., Ersayın, S., Gülsoy, Ö.Y., Ekmekçi, Z., Can, M., Asian, A., 2000. Modelling and simulation of grinding circuit at Çayeli Bakır İşletmeleri A.Ş. (ÇBİ) flotation plant, *Mineral Processing on the Verge of the 21st Century*, Özbayoğlu et al. (eds), A.A. Balkema Publishers, pp65-70.